Effects of linker sequence modifications on the structure, stability and biological activity of a cyclic α-conotoxin

Bodil B. Carstens[1,2#], Joakim Swedberg[1#], Géza Berecki[3], David J. Adams[3], David J. Craik[1], Richard J. Clark[2*]

[1] Institute for Molecular Bioscience, The University of Queensland, Brisbane, Queensland, 4072, Australia

[2] School of Biomedical Sciences, The University of Queensland, Brisbane, Queensland, 4072, Australia

[3] Health Innovations Research Institute, RMIT University, Melbourne, Victoria 3083, Australia

[#] contributed equally

[*]Address correspondence to: Dr. Richard J Clark, The University of Queensland, School of Biomedical Sciences, Brisbane, QLD, 4072, Australia. Phone: +61 7 3365 1527. Fax: +61 7 3365 1766. Email: richard.clark@uq.edu.au

D.J. Adams current affiliation: Illawarra Health and Medical Research Institute, University of Wollongong, Wollongong, NSW 2522, Australia Email: djadams@uow.edu.au

Keywords: conotoxins, cyclic peptides, drug design, membrane permeability, structure-function.

Abstract

The cyclic conotoxin analogue cVc1.1 is a promising lead molecule for the development of new treatments for neuropathic and chronic pain. The design of this peptide includes a linker sequence that joins the N and C termini together, improving peptide stability while maintaining the structure and activity of the original linear Vc1.1. The effect of linker length on the structure, activity and stability of cyclised conotoxins has been studied previously but the effect of altering the composition of the linker sequence has not been investigated. In this study, we designed three analogues of cVc1.1 with linker sequences that varied in charge, hydrophobicity and hydrogen bonding capacity and examined the effect on structure, stability, membrane permeability and biological activity. The three designed peptides were successfully synthesized using solid phase peptide synthesis approaches and had similar structures and stability compared with cVc1.1. Despite modifications in charge, hydrophobicity and hydrogen bonding potential, which are all factors that can affect membrane permeability, no changes in the ability of the peptides to pass through membranes in either PAMPA or Caco-2 cell assay were observed. Surprisingly, modification of the linker sequence was deleterious to biological activity. These results suggest the linker sequence might be a useful part of the molecule for optimisation of bioactivity and not just the physiochemical properties of cVc1.1.

Introduction

Conotoxins are disulfide-rich peptides from the venom of marine snails of the *Conus* genus that range in size from 10–30 amino acids including two or more disulfide bonds.[1,2] Despite the small size of conotoxins, there is vast potential for diversity, including sequence variation and different disulfide bond frameworks[3,4]. This sequence and structural diversity results in individual conotoxins being potent and specific ligands for their particular pharmacological target, which includes voltage-gated sodium, calcium and potassium channels, nicotinic acetylcholine receptors (nAChRs), the norepinephrine transporter (NET), and G protein-coupled receptors.[1,2,5,6] Many of these targets are in neurological pathways involved in pain transmission and hence conotoxins are valuable as leads for drug development and as research tools for mechanistic studies. However, despite the fact that conotoxins are highly potent and selective, there are a number of limitations associated with peptides as drugs; they have low membrane permeability so have limited oral availability and they are typically rapidly degraded *in vivo* by plasma and tissue peptidases.

As conotoxins are small peptides, they are ideally suited for chemical synthesis using solid phase peptide synthesis approaches, which makes them amenable to incorporation of chemical modifications to improve *in vivo* efficacy. A number of studies have focused on improving conotoxin stability with the aim of enhancing the biopharmaceutical properties of conotoxins through chemical modification. Strategies used have included the introduction of a cyclic backbone[7-16], substitution of cysteine with selenocysteine[14,17-23], lipidation[24-26] and incorporation of non-peptidic backbone spacers.[27]

Our research focus has been on the backbone cyclization of α-conotoxins as a method of stabilisation against proteolytic degradation. The α-conotoxins range in size from approximately 8–22 residues and contain two disulfide bonds in a Cys^{I}-Cys^{III} and Cys^{II}-Cys^{IV} connectivity. The spacing of the cysteine residues defines two loop regions (loops 1 and 2) that vary in composition

and length, which are stabilised into a helical structure by the disulfide bonds. Subclasses of α-conotoxins are defined by the number of residues in each of these loop regions, for example, a 4/7 α-conotoxin contains four residues in loop 1 and seven in loop 2. The α-conotoxins are potent antagonists of nicotinic acetylcholine receptors (nAChR) and recently a subset of α-conotoxins has been shown to inhibit high voltage- activated calcium channels via a γ-aminobutyric acid type B ($GABA_B$) receptor-dependent mechanism.[28,29] Our initial work focused on the cyclization of the 4/7 α-conotoxin MII where we demonstrated the feasibility of the approach by producing a cyclic variant of MII by introducing a short sequence of glycine and alanine residues to link the N and C termini[13]. An MII analogue cyclized using a 5-residue linker had a distorted structure and reduced biological activity, whereas cyclic MII analogues with 6- or 7- residue linkers possessed a structure, potency and selectivity consistent with the linear wild-type conotoxin.

Several other studies have investigated the effect of linker length on the activity and stability of cyclized α-conotoxins from other subclasses. A study on the cyclization of the 4/3 α-conotoxin ImI used short linker sequences of one to three amino acids, which resulted in preferential formation of a less active non-native disulfide isomer.[15] Two studies on the backbone cyclization of the 4/6 α-conotoxin AuIB also examined the influence of linker length upon oxidative folding of AuIB.[7,14] A 5-residue linker provided the highest yield of the native 'globular' disulfide isomer (Cys^{I}-Cys^{III}, Cys^{II}-Cys^{IV}), whereas a 1-, 3- or 4-residue linker resulted predominantly in the alternative "ribbon" isomer (Cys^{I-IV}, Cys^{II-III}). Cyclic AuIB analogues with 4–7 residues and the globular disulfide connectivity displayed the native structure based on NMR studies, but the disorder in the linker increased with its length. The globular isomer with the 4-residue linker was produced using selective protection of the cysteine residues, and resulted in the highest activity at the α3β4 nAChR subtype.[7] However, Armishaw *et al.*[14] reported that a 2-residue linker was the most potent at the α3β4 nAChR subtype although a detailed structural analysis was not done on this peptide.

A study on the 4/3 α-conotoxin RgIA investigated the effect of backbone cyclisation using linkers ranging in length from 3–7 residues.[10] Linker lengths of 5–7 residues resulted in little structural perturbation as determined by NMR spectroscopy and these analogues were also the most biologically active. Finally, we designed an orally active analgesic cyclic conotoxin based on the 4/7 α-conotoxin Vc1.1.[12] The N- and C-termini of Vc1.1 are 12 Å apart and based on previous cyclization studies of conotoxins and other disulfide-rich peptides, we predicted that a linker length of 5–6 residues would be effective at spanning the termini and retain activity. Only the 6-residue linker retained activity and showed increased stability in simulated gastric fluid, intestinal fluid and human serum over the parent acyclic peptide. Importantly, the cyclic analogue with a 6-amino acid linker was orally active in a rat model of neuropathic pain and was 120 times more potent than gabapentin.

All of the studies on the cyclization of conotoxins have used linker sequences comprising alanine and glycine residues as they are considered biologically "inert" and glycine offers additional conformational flexibility. To date, little is known about how linker composition might affect the structure, stability and biological activity of backbone cyclized conotoxins. A cyclic derivative of the χ-conotoxin MrIA, an inhibitor of the noradrenaline transporter, was developed using a RGD sequence to link the N and C termini.[11] This cyclic peptide both blocked noradrenaline uptake and inhibited aggregation of platelet-rich human plasma. Interestingly, the cyclic MrIA RGD peptide was also more stable in rat plasma than a cyclic MrIA analogue with an Ala-Gly linker. Most recently, we described the cyclization of the P-superfamily conotoxins gm9a and bru9a, which contain three disulfide bonds in a cystine knot arrangement and are topologically similar to the cyclotide family of cyclic peptides.[16,30] Using a GLP linker sequence, based on the structurally analogous loop in the cyclotide kalata B1, cyclic analogues of gm9a and bru9a that were

structurally almost identical to the linear parent peptides were produced.[16]

In this study, we further investigate the role of linker composition on the structure, stability, activity and pharmaceutical properties of cyclic conotoxins. Using the cyclic analogue of α-conotoxin Vc1.1 as a model peptide, we used molecular dynamics simulations to redesign the linker sequence with the aim of improving membrane permeability and structural stability. Following chemical synthesis and structural characterization of the new cyclic Vc1.1 analogues, we investigated the effects of these linker changes on biological activity *in vitro* and on membrane permeability in both PAMPA and CACO-2 assays.

Materials and Methods

Materials

Peptide resins, amino acids and reagents were purchased from Chem-Impex International Inc. (Wood Dale, IL) and Chempep Inc (Wellington, FL). Human male AB serum was purchased from Sigma-Aldrich. Caco-2 cells were kindly provided by Prof. Istvan Toth, The University of Queensland. All cell culture reagents were purchased from Gibco, Life Technologies and Invitrogen. Lucifer yellow solution was purchased from Sigma-Aldrich and culture plates were purchased from Corning Incorporated. Parallel artificial membrane permeability assay (PAMPA) plates were obtained from BD Biosciences (North Ryde, NSW).

Linker design by molecular dynamics

The solution NMR structure of linear Vc1.1 (PDB ID: 2H8S) was used as a template, and cVc1.1 and linker analogues were constructed using YASARA Dynamics 13.4.24.[31] CHARMM topologies and parameters for N-methyl groups were calculated using the SwissParam web server[32] while

those for acetonitrile were obtained from CGenFF 2b8.[33] Systems were solvated with TIP3P water and neutralized by Na^+/Cl^- counter ions in VMD 1.9.2.[34] This procedure generated systems of ~10,000 atoms. Each system was equilibrated using a stepwise relaxation procedure using NAMD 2.10[35] as previously described.[36] Production simulation runs of 15 ns were performed for each compound and simulation snapshots were saved every 5 000 steps producing 15 000 frames for analysis. The average simulation structure was chosen as the frame that most closely aligned with the average simulation coordinates.

The polar surface areas (PSA), surface areas (SA) and virtual log n-octanol/water partition coefficients (vLogP) were calculated in VEGA ZZ 3.0.5[37] from the simulation trajectories for cVc1.1-L1, cVc1.1-L2, and cVc1.1-L3, while these parameters for atenolol (PubChem CID 2249) and quinidine (PubChem CID 441074) were calculated from their respective known structures.

Synthesis and oxidative folding

All three peptides were synthesised on PAM-Gly resin by solid phase peptide synthesis[38] using a CS Bio Synthesizer (CS 336X; Menlo Park, CA). S-trityl-β-mercaptopropionic and the first amino acid were coupled manually. All peptides were synthesized using Boc chemistry with an *in situ* neutralization/*O*-benzatriazole-*N, N, N', N'* - tetramethyluronium hexafluorphosphate (HBTU) protocol.[39] The side chains of Cys^{II} and Cys^{IV} were protected with acetamidomethyl (Acm) groups to facilitate regioselective disulfide bond formation. Peptides were cleaved from resin using hydrofluoric acid (HF) with *p*-cresol as a scavenger (12:1.5 v/v). The reaction was allowed to proceed at -5 to 0 °C for 1.5 h. The HF was removed under vacuum and the peptide was precipitated in ether, filtered and solubilized in 50% acetonitrile containing 0.05% trifluoroacetic acid (TFA), and lyophilized.

The crude peptides were purified by reverse phase-HPLC on a Phenomenex C_{18} column using a gradient of 0–50% B (Buffer A: H_2O/0.05% TFA; Buffer B: 90% CH_3CN/10% H_2O/0.045% TFA)

in 50 min, with the eluent monitored at 215/280 nm. ESI-MS confirmed the molecular mass of the synthesized peptide, which was lyophilized before a two-step oxidation protocol was employed. The reduced peptides were first oxidized in 0.1 M NH_4HCO_3 buffer (pH 8.2) at a concentration of 0.3 mg/ml overnight at room temperature and subsequently purified by RP-HPLC using a gradient of 0–50% buffer B in 50 min. The second disulfide bridge was formed by treatment of the peptides with iodine under acidic conditions. The peptides were dissolved in buffer A (1 mg/ml) followed by slow addition of I_2 in CH_3CN until solution became yellow/dark brown. The reaction mixture was then stirred for 15 min at 37°C before it was quenched by addition of ascorbic acid until the mixture became colorless. The completely oxidized peptides were purified by RP-HPLC on a 0.5% gradient, and analytical RP-HPLC and ESI-MS confirmed the purity and molecular mass of the peptides. Peptide concentration was determined by measuring absorbance at 280 nm and using the Beer-Lambert law. The molar extinction coefficients were predicted based on the content of tryptophan, tyrosine and cystines.[40]

NMR spectroscopy

NMR data were acquired on a Bruker Avance 600 MHz NMR spectrometer equipped with a cryoprobe. cVc1.1-L1 and L3 were dissolved in 90% H_2O/10% D_2O (pH 3.1) and cVc1.1-L2 was dissolved in 50% CH_3CN/40% H_2O/10% D_2O (pH 2.5) to a final concentration of 1 mg/ml. 2,2-dimethyl-2-silapentane-5-sulphonate (DSS) was added as a chemical shift reference (0.0 ppm). Two-dimensional spectra for all peptides were recorded at 280 K and processed by Topspin 2.1 (Bruker). Datasets recorded included homonuclear spectra TOCSY (4–8 scans) with a mixing time of 80 ms and NOESY (24–54 scans) with a mixing time of 200 ms, and analyzed using CCP NMR software.[41] Spectra were recorded with a spectral width of 12 ppm, and a resolution of 4k data points in the f2 dimension and 512 increments in the f1 dimension. Spectra were assigned using the sequential assignment protocol[42] and secondary shifts calculated using the random coil values

reported by Wishart *et al*..[43] For *N*-methylated amino acids random coil values for the unmethylated residue were used.

Caco-2 permeability

Caco-2 cells were maintained in Dulbecco's modified Eagle's medium supplemented with 10% fetal bovine serum, 1% non-essential amino acids and 1% penicillin-streptomycin and maintained at 37 °C in 5% CO_2 and 90% relative humidity. Cells were seeded when ~90% confluent in 12-well membrane plates (PET membrane, 1.12 cm^2 growth area, 0.4 μM pore size) at ~50 000 cells/well, and cultured for 21 days in order to create the monolayer with media changed every two days. Passages 37−48 were used for the experiments. The integrity of the Caco-2 cell monolayer was tested by measuring the trans epithelial electrical resistance (TEER) values using an EVOM Millicell® ERS-2 voltmeter (Millipore Co.). Following 21 days in cell culture, monolayers developed TEER values of 250–400 Ω cm^2, which is consistent with an intact cell monolayer. The permeability of the monolayer was also tested using Lucifer yellow by measuring the absorption of Lucifer yellow at the end of assay. If >1% Lucifer yellow was absorbed, the cell monolayer was shown to no longer be intact and hence results could not be interpreted.

On the day of assay, media was aspirated off and cells washed with Hank's Buffered Saline Solution (HBSS) containing 1.25 mM $CaCl_2$ and 0.5mM $MgCl_2$ (pH 7.4). After, cells were left in fresh HBSS solution for 30 min under shaking (55 rpm) at 37°C and TEER values were measured. Samples were prepared to a concentration of 50 μM in HBSS with 10 μM Lucifer yellow containing solutions, and added to the apical side of the monolayer. Plates were returned to a shaking incubator (55 rpm), and 100 μl taken from both basolateral and apical sides after 45 and 90 min of incubation to be analyzed for peptide content. 200 μl samples were also taken from both basolateral and apical sides after 90 min of incubation for Lucifer yellow absorbance readings to confirm monolayer integrity. After 90 min the volumes of the compartments were replenished with HBSS solution to

starting volumes, and TEER measurements were repetitively recorded to confirm that the monolayer was not breached during assay. Atenolol and quinidine were used as negative and positive controls, respectively. Samples were analyzed using LC-MS and apparent permeability coefficients (P_{app}) calculated using equation (1):

$$P_{app} = \frac{1}{Area * C_D(0)} * \frac{dM_r}{dt} \qquad (1)$$

where *Area* is the surface of the cell monolayer (1.12cm^2), $C_D(0)$ is the initial concentration of the compound applied to the donor chamber, *t* is the time (s), M_r is the mass of compound in the receiver compartment, and dM_r/dt is the flux of the compound across the monolayer.

Each peptide was tested in triplicate (3 wells) and repeated 3 times. Peptides were kept in 5 mM DMSO and stored at –20°C in between assays.

Parallel Artificial Membrane Permeability Assay (*PAMPA)*

PAMPA studies were carried out in 96-well filter plates pre-coated with a lipid-oil-lipid tri-layer artificial membrane (BD Gentest™). Before use, the PAMPA plate was warmed to room temperature for 30 min. Samples were prepared to a concentration of 50 μM in HBSS with 5% DMSO. 300 μl was added to the donor compartments (receiver plate) and the acceptor compartments were filled with 200 μl HBSS buffer (filter plate).

The filter plate was coupled with the receiver plate and the resulting construct was covered in aluminium foil and incubated at room temperature for 5 h. At the end of the incubation, the plates were separated and the final concentrations of compounds were determined by LC-MS. Each peptide was tested in triplicate and repeated twice. Peptides were kept in 5 mM DMSO and stored at –20°C in between assays. The permeability (P_e) was calculated according to the equation in units of cm/s:

Permeability (cm/s): $P_e = \{-\ln[1-C_A(t)/C_{eq}]\}/A*(1/V_D+1/V_A)*t]$

where A is the filter area (0.3 cm^2), V_D and V_A represent the donor well volume (0.3 ml) and the acceptor well volume (0.2 ml), respectively, t is the incubation time in s, $C_A(t)$ is the compound concentration in acceptor well at time t (mM), C_D (t) is the compound concentration in donor well at time t (mM) and

$C_{eq} = [C_D(t)*V_D+C_A(t)*V_A]/(V_D+V_A)$

Serum stability

Serum stability assays were carried out on male AB human serum (Sigma-Aldrich). Two different protocols were employed, one using solid phase extraction cartridges; serum was thawed at 37°C for 20 min before peptide (1 mg/ml in H_2O) was added and vortexed (98:2 v/v). 100 µl samples were removed at 0, 2, 4, 6, 8, 10, 12 and 24 h and added to 900 µl 100 mM ammonium acetate (pH 3.0) to deactivate serum enzymes before incubated on ice for 30 min. Peptides were recovered using solid phase extraction cartridges (Phenomenex 60 mg Strata-X polymeric RP cartridges (8B-S100-UBJ)). First, the cartridge was washed with 6 ml methanol, followed by 3 ml 70% CH_3CN: 1% formic acid and then 3 ml 1% formic acid to equilibrate the column. Samples were then added to the cartridge and washed with 3 ml 1% formic acid before it was eluted with 1.5 ml of the appropriate CH_3CN concentration and 1% formic acid. The eluted fractions were lyophilized and redissolved in 100 µl 1% formic acid before recovery was calculated by LC-MS on a Vydac C_{18} column using a 2% gradient. Recovery was calculated based on the peak area for the corresponding $[M+2H]^{2+}$ ion. Vc1.1 and cVc1.1 were used as controls.

Primary Culture of dorsal root ganglion (DRG) Neurons and Patch-Clamp Recordings

DRG neurons were enzymatically dissociated from ganglia of 4−16-days-old Wistar rats as described previously[29] and used for experiments within 24–48 h. Cells were transferred into a small-volume (~200 µl) recording chamber constantly perfused with a solution containing (in mM): 150 tetraethylammonium chloride (TEA-Cl), 2 $CaCl_2$, 10 D-glucose, 10 HEPES, pH 7.4 (with NaOH). Borosilicate glass electrodes were filled with an internal solution containing (in mM): 140 CsCl, 1 $MgCl_2$, 5 MgATP, 0.1 Na-GTP, 5 BAPTA-Cs_4, 10 HEPES, pH 7.3 (with CsOH) and had resistances of 1.5−2.5 MΩ. Patch-clamp recordings were performed with a Multiclamp 700B amplifier controlled by Clampex9.2/DigiData1332 acquisition system (Molecular Devices), at room temperature (23–25°C). In DRG neurons, calcium channel currents (I_{Ca}) were evoked by depolarizing voltage steps of 100 ms duration from a holding potential of −80 mV. Currents were filtered at 2 kHz and sampled at 5 kHz. Leak and capacitive currents were subtracted using a −P/4 pulse protocol. Data are mean ± SEM (n, number of experiments).

Results and Discussion

Linker design/molecular dynamics

The previously described cyclization linker sequence of cVc1.1 contains a series of Gly and Ala residues (Figure 1, Table 1). We investigated how modulating the linker sequence of cVc1.1 would affect stability, permeability and activity of this cyclic conotoxin. *N*-methylation of amino acids in peptides is a common strategy for increasing their hydrophobicity. Since *N*-methylation can have unforeseen consequences for peptide conformation, cVc1.1 and *N*-methylated linker variants were investigated by molecular dynamics. Ideally, compounds of interest would be simulated with their target but there was no available structure of the $GABA_B$ receptor and the binding site of cVc1.1 is unknown, so the analogues were simulated in solution for comparison to cVc1.1 using the α-carbon Root-Mean-Square Deviation (RMSD) and intramolecular hydrogen bond patterns. Compounds

with more intramolecular hydrogen bonds have less polar groups on their surface to interact with water and thus reduce the polarity of the compound.[44]

Each of the six residues of the cyclisation linker in cVc1.1 was sequentially modelled as *N*-methylated to investigate any effects on the conformation and secondary structure of the peptide scaffold. The molecular dynamics simulations suggested that *N*-methylation was structurally well tolerated at any position in the linker since the average structure of the variants deviated from cVc1.1 with α-carbon RMSD values in the 0.31-0.8 Å range (Table 1).

Satisfied that the whole linker sequence was amendable to *N*-methylation, we designed a series of 14 variants with linkers having diverse biophysical properties based on basic, hydrophobic or acidic residues (Table 1). The linkers included Gly residues strategically placed in the sequence to aid NMR assignment. To explore the effect on membrane permeability by positively charged, hydrophobic or acidic residues, three linkers, one from each of the three groups, was chosen to be synthesized based on having the lowest α-carbon RMSD compared to cVc1.1 during molecular dynamics: GK**G**KGK (cVc1.1-L1, Figure 2B, residues highlighted in **bold** being *N*-methylated), G**V**G**V**GV (cVc1.1-L2, Figure 2C) and GE**G**E**G**E (cVc1.1-L3, Figure 2D). cVc1.1-L2 and cVc1.1-L3 had both the lowest α-carbon RMSD and the most number of hydrogen bonds within their groups. cVc1.1-L1 had the lowest α-carbon RMSD and the second most intermolecular hydrogen bonds, and the choice was made on the rationale that structural similarity to cVc1.1 was the most important factor.

Synthesis and oxidative folding

The cyclic analogues were assembled using solid phase peptide synthesis on a CS Bio Synthesizer (336X) with Boc/HBTU chemistry. A previous study showed that random oxidation of cVc1.1 gave rise to both the ribbon and the globular isomers[12] therefore a selective disulfide bond strategy was

used to produce the cVc1.1 analogues. This involved incorporating Acm protecting groups to facilitate selective formation of the Cys^{I}-Cys^{III} and Cys^{II}-Cys^{IV} disulfide bonds corresponding to the native disulfide isomer. The disulfide bonds were formed in two steps under different conditions; the first disulfide bond between Cys^{I}-Cys^{III} was formed in ammonium bicarbonate buffer at room temperature stirring overnight followed by RP-HPLC purification. The second disulfide bond between Cys^{II}-Cys^{IV} was formed by removal of the Acm protecting groups and subsequent oxidation in the presence of iodine under acidic conditions. As expected, only the globular isomer was observed after folding using this procedure. The fully oxidized peptides were purified by RP-HPLC, and analytical RP-HPLC and ESI-MS were used to characterize the oxidized peptides (Figure 2). ESI-MS of the fully oxidized peptides revealed $[M+2H]^{2+}$ to be 1180.4 Da for cVc1.1-L1 (calculated 1179.8 Da), 1143.8 for cVc1.1-L2 (calculated 1143.2 Da) and 1180.7 Da for cVc1.1-L3 (calculated 1188.2).

NMR analysis

The purified peptides were analyzed by NMR spectroscopy to confirm the globular α-conotoxin fold. All three analogues gave well-dispersed ^{1}H NMR spectra indicating that they adopt ordered structures and were further analyzed by two-dimensional NMR. The assignment of the proton chemical shifts was done using standard methods[42]. Briefly, NH-NH_{i+1}, Hα-NH_{i+1} and Hβ-NH_{i+1} connectivities obtained from the NOESY spectra were used in the sequential assignment of individual spin systems determined from the TOCSY spectra. Sequential Hα-NH_{i+1} connectivities were observed for almost the entire peptide chains, except at Pro6 and Pro13 as these residues lack amide protons. Both prolines were in the *trans* configuration for all analogues as indicated by intense Hα-Hδ NOEs between the preceding residue and the Pro, which matches the data for cVc1.1 and Vc1.1. Although cVc1.1-L2 and L3 were chemically pure as evaluated by HPLC and MS, extra spin systems were present in their NMR spectra, suggesting the presence of a second conformation in solution. However, this conformer was only observed for a few residues on either side of Pro13,

which is likely due to proline cis/trans isomerization but this could not be confirmed, as the conformer could not be fully assigned due to lack of NOEs. Observation of minor conformations in solution for small disulfide-rich peptides is not uncommon, and has been reported for other α-conotoxins, including AuIB.[45]

Analysis of the secondary shifts can supply information on the secondary structural elements present in peptides[46]. Secondary shifts are the differences between observed Hα shifts and the random coil Hα shifts for the corresponding residues. For example, a series of negative secondary Hα shifts suggest an α-helix, which is characteristic for α-conotoxins. Figure 4A shows the secondary αH chemical shifts for the synthesized analogues and cVc1.1 indicating negative secondary shifts between Gly1−Cys4 and Pro6−Asp11. Negative secondary Hα shifts between Pro 6−Asp11 have been reported previously for both Vc1.1 and cVc1.1[12,47] displaying an α-helix in this region of the peptide. The analogues follow the same pattern in shifts as cVc1.1 illustrating the high degree of structural similarity between the analogues and cVc1.1, which in turn indicates that the analogues might have similar bioactivity as cVc1.1. However, there are some variations in the linker region, which is due to different linker residues. It should be noted that the data for cVc1.1-L2 was acquired in 50% acetonitrile, as the peptide was not soluble in 90%H_2O/10%D_2O, which might explain some of the differences in secondary αH shifts for this analogue compared to the parent peptide. To investigate the effect of the solvent on the structure of cVc1.1-L2, this compound was modelled in 50% acetonitrile. Consistent with the secondary shifts, the average structure of cVc1.1-L2 in 50% acetonitrile deviated more from cVc1.1 (α-Carbon RMSD = 0.69 Å) than the same compound in water (α-Carbon RMSD = 0.26 Å) (Figure 4B).

Permeability assays

Caco-2 studies were undertaken to investigate if the chemical properties of the analogues could modify the absorption of the α-conotoxin. The human intestinal Caco-2 cell line represents an

established *in vitro* model of the intestinal barrier to study the absorption and metabolism of drugs[48]. Such permeability assays can be used to mimic both the intestinal environment and the blood brain barrier and have been shown to correlate to human intestinal absorption.[49-51] Table 2 shows that cVc1.1-L2 tested at a concentration of 50 μM exhibited low permeability, comparable to that seen for atenolol, which was applied as a passive paracellular marker and displayed permeability (P_{app} <1 x 10^6 cm/s) consistent with the literature.[52-55] cVc1.1, cVc1.1-L1 and cVc1.1-L3 were not permeable in this assay at a concentration of 50 μM, whereas quinidine, applied as a high permeable marker, had permeability values similar to those reported in the literature.[52,56,57] A comparison of the calculated biophysical properties of cVc1.1-L2 with cVc1.1, cVc1.1-L1 and cVc1.1-L3 showed that cVc1.1-L2 had the smallest polar surface area (PSA) and the highest lipophilicity (as indicated by vLogP), consistent with cVc1.1-L2 being more permeable (Table 2).

PAMPA determines the permeability of substances from a donor compartment, through a lipid-infused artificial membrane into an acceptor compartment. Similar to the Caco-2 assay, it is used as a high-throughput screening technique. However, PAMPA is solely intended to measure the intrinsic ability of compounds to permeate lipophilic barriers (at pH 7.4) as a guide to the possibility of passive absorption through the gut wall. Unlike Caco-2 cells, the assay is not complicated by influx or efflux mechanisms, or for substances to be absorbed via the paracellular route. As shown in Table 2, cVc1.1-L1 was not permeable in the PAMPA system at a concentration of 50 μM, which suggests that it is not passively absorbed through the intestine, whereas cVc1.1, cVc1.1-L2 and L3 displayed low permeability. These findings are consistent with cVc1.1-L1 having the lowest vLogP (Table 2) and a charge of +4 at physiological pH, compared to a charge of +1 for the other linker variants.

PAMPA and Caco-2 cell assays are the most frequently used high-throughput systems for screening of drug absorption of compounds in the early stages of drug discovery. Although the linker

analogues and cVc1.1 were tested in both systems and were not permeable in these *in vitro* permeability assays, this might not translate to *in vivo* models. For example, cyclosporine A, which has an oral bioavailability of 20-40% only has a P_{app} of 1 x 10^6 in the apical to basal direction of the Caco-2 assay[58] and 1.1 x 10^6 in RRCK cells.[59] Therefore, animal pharmacokinetic studies of cVc1.1 and linker analogues are required to fully understand the bioavailability of these peptides.

Peptide stability

The three linker analogues were tested in human serum to determine the effects of the new linker sequences on peptide stability. Figure 5 shows that cVc1.1-L3 is the most stable of the linker analogues, and cVc1.1-L2 the least stable. At the 24 h time point, there was 73.5 ± 12.3%, 68.6 ± 9.4% and 91.6 ± 0.3% of cVc1.1-L1, cVc1.1-L2 and cVc1.1-L3 remaining in human serum, respectively (n = 9, from three separate experiments). For all analogues, two peaks corresponding to the same mass of the individual linker analogues were observed after 2−4 h incubation at 37°C, suggesting some re-shuffling of the disulfide bonds in serum. Linear Vc1.1 and cVc1.1 were used as controls. cVc1.1 has been reported to be more stable in human serum than its linear analogue Vc1.1[12], which is consistent with the present study. Additionally, cVc1.1-L3 (91.6 ± 0.3%) was slightly more stable in human serum than the parent peptide (86.4 ± 4.2%). Previous studies[7,8,10-15] have shown that backbone cyclization of disulfide-rich peptides is an effective approach for improving resistance to proteolysis. Typically the linker sequences used in these studies have been constructed from functionally inert residues like Ala or Gly and NMR studies have revealed that they are usually unstructured in solution.[7,10,12,13] Modification of the linker residues to more biologically functional residues, such as the charged amino acids used in cVc1.1-L1 and L3, might introduce additional protease cleavage sites into the peptide negating the benefits of backbone cyclisation. However, this could be counteracted by reduced flexibility of the linker sequence, which is likely to reduce susceptibility to proteolysis. Our results showed that cVc1.1-L1 and L2, containing positively charged and hydrophobic residues, were the least stable analogues when

compared to cVc1.1 and cVc1.1-L3. As the NMR secondary shift analysis revealed that the αH secondary shifts of the linker residues for all analogues approximated random coil values we would predict that the differences is stability between the peptides is due to the residue composition of the linkers in cVc1.1-L1 and L2 being more susceptible to proteolysis rather than the cVc1.1 and cVc1.1-L3 linkers providing greater structural rigidity. Consequently, future studies aiming at stabilising peptides by linker cyclization may benefit from exploring more diverse amino acid functionalities to better understand the balance between linker functionality and rigidity.

Biological activity

The three linker analogues were tested for their effect on high voltage-activated (HVA) calcium channel currents (I_{Ca}) in rat DRG neurons. All peptides were tested at a concentration of 500 nM because in rat DRG neurons, the half-maximal inhibitory concentration of cVc1.1 is ~0.3 nM and 500 nM of Vc1.1 was shown to be maximally effective for N-type I_{Ca} inhibition.[12] Figure 6 shows that cVc1.1-L1 (500 nM) inhibited a relatively small amount of I_{Ca}, whereas cVc1.1-L2 and L3 did not affect I_{Ca}. Subsequent application of the selective $GABA_BR$ agonist baclofen or cVc1.1 as positive controls, resulted in a further inhibition of I_{Ca} (Figure 6B). Figure 6C shows a bar graph of the averaged relative peak I_{Ca} amplitudes in the presence of cVc1.1-L1, L2, L3, and baclofen compared to control. cVc1.1-L1 (500 nM) inhibited I_{Ca} by 6.8 ± 1.3% whereas baclofen (50 μM) inhibited I_{Ca} by 34.9 ± 4%. Although the substitutions in cVc1.1-L3 that introduced carboxylic acid groups made large changes to the polarity and dipole moment of the molecule that may interfere with receptor binding, it is difficult to rationalize why the conservative substitutions in cVc1.1-L2 abolished the activity. However, since cVc1.1-L2 was not water soluble, it is possible that the delivery of the compound to DRG neurons in a water-based buffer system might not be optimal, and the cVc1.1-L2 concentration under these conditions could not be estimated with confidence.

Conclusions

In this study the cyclization linker sequence for α-conotoxin cVc1.1 was modified to improve the peptide's stability and pharmacokinetic properties. All linker analogues were found to be structurally similar to cVc1.1 and relatively stable in human serum but all had low membrane permeability. Surprisingly, despite their structural similarity to cVc1.1, none of the linker analogues appreciably inhibited HVA calcium channel currents in DRG neurons. This finding suggests that future studies should focus on the role of the linker region in modulating both the activity of cVc1.1 as well as its pharmacological properties.

Acknowledgements

We thank Mr. Phil Sunderland for peptide synthesis, and Dr. Susan Northfield, Ms. Stephanie Chaousis and Mrs. Barbara Colless, who supported the CACO-2 cell and PAMPA assays. This work was supported by National Health & Medical Research Council (NHMRC) Project Grants (631457, APP1076136 to DJA and RJC, and APP1034642 to GB and RJC). BBC was supported by a University of Queensland International Scholarship and a University of Queensland Research Scholarship, JS by an NHMRC Early Career Fellowship, DJC by an NHMRC Senior Principal Research Fellowship and RJC by an ARC Future Fellowship.

References

1. Olivera, B. M.; Showers Corneli, P.; Watkins, M.; Fedosov, A. Annu Rev Anim Biosci 2014, 2, 487-513.
2. Akondi, K. B.; Muttenthaler, M.; Dutertre, S.; Kaas, Q.; Craik, D. J.; Lewis, R. J.; Alewood, P. F. Chem Rev 2014, 114, 5815-5847.
3. Kaas, Q.; Westermann, J. C.; Craik, D. J. Toxicon 2010, 55, 1491-1509.
4. Kaas, Q.; Yu, R.; Jin, A. H.; Dutertre, S.; Craik, D. J. Nucleic Acids Res 2012, 40, D325-330.
5. Lewis, R. J.; Dutertre, S.; Vetter, I.; Christie, M. J. Pharmacol Rev 2012, 64, 259-298.
6. Carstens, B. B.; Clark, R. J.; Daly, N. L.; Harvey, P. J.; Kaas, Q.; Craik, D. J. Curr Pharm Des 2011, 17, 4242-4253.
7. Lovelace, E. S.; Gunasekera, S.; Alvarmo, C.; Clark, R. J.; Nevin, S. T.; Grishin, A. A.; Adams, D. J.; Craik, D. J.; Daly, N. L. Antioxid Redox Signal 2011, 14, 87-95.
8. Lovelace, E. S.; Armishaw, C. J.; Colgrave, M. L.; Wahlstrom, M. E.; Alewood, P. F.; Daly, N. L.; Craik, D. J. J Med Chem 2006, 49, 6561-6568.
9. Jia, X.; Kwon, S.; Wang, C. I.; Huang, Y. H.; Chan, L. Y.; Tan, C. C.; Rosengren, K. J.; Mulvenna, J. P.; Schroeder, C. I.; Craik, D. J. J Biol Chem 2014, 289, 6627-6638.
10. Halai, R.; Callaghan, B.; Daly, N. L.; Clark, R. J.; Adams, D. J.; Craik, D. J. J Med Chem 2011, 54, 6984-6992.
11. Dekan, Z.; Wang, C. I.; Andrews, R. K.; Lewis, R. J.; Alewood, P. F. Org Biomol Chem 2012, 10, 5791-5794.
12. Clark, R. J.; Jensen, J.; Nevin, S. T.; Callaghan, B. P.; Adams, D. J.; Craik, D. J. Angew Chem Int Ed Engl 2010, 49, 6545-6548.
13. Clark, R. J.; Fischer, H.; Dempster, L.; Daly, N. L.; Rosengren, K. J.; Nevin, S. T.; Meunier, F. A.; Adams, D. J.; Craik, D. J. Proc Natl Acad Sci U S A 2005, 102, 13767-13772.

14. Armishaw, C. J.; Jensen, A. A.; Balle, L. D.; Scott, K. C.; Sorensen, L.; Stromgaard, K. Antioxid Redox Signal 2011, 14, 65-76.

15. Armishaw, C. J.; Dutton, J. L.; Craik, D. J.; Alewood, P. F. Biopolymers 2010, 94, 307-313.

16. Akcan, M.; Clark, R. J.; Daly, N. L.; Conibear, A. C.; de Faoite, A.; Heghinian, M. D.; Sahil, T.; Adams, D. J.; Mari, F.; Craik, D. J. Biopolymers 2015, 104, 682-692.

17. Zhang, M. M.; Han, T. S.; Olivera, B. M.; Bulaj, G.; Yoshikami, D. Biochemistry 2010, 49, 4804-4812.

18. Walewska, A.; Zhang, M. M.; Skalicky, J. J.; Yoshikami, D.; Olivera, B. M.; Bulaj, G. Angew Chem Int Ed Engl 2009, 48, 2221-2224.

19. Muttenthaler, M.; Nevin, S. T.; Grishin, A. A.; Ngo, S. T.; Choy, P. T.; Daly, N. L.; Hu, S. H.; Armishaw, C. J.; Wang, C. I.; Lewis, R. J.; Martin, J. L.; Noakes, P. G.; Craik, D. J.; Adams, D. J.; Alewood, P. F. J Am Chem Soc 2010, 132, 3514-3522.

20. Green, B. R.; Zhang, M. M.; Chhabra, S.; Robinson, S. D.; Wilson, M. J.; Redding, A.; Olivera, B. M.; Yoshikami, D.; Bulaj, G.; Norton, R. S. FEBS J 2014, 281, 2885-2898.

21. Gowd, K. H.; Blais, K. D.; Elmslie, K. S.; Steiner, A. M.; Olivera, B. M.; Bulaj, G. Biopolymers 2012, 98, 212-223.

22. de Araujo, A. D.; Callaghan, B.; Nevin, S. T.; Daly, N. L.; Craik, D. J.; Moretta, M.; Hopping, G.; Christie, M. J.; Adams, D. J.; Alewood, P. F. Angew Chem Int Ed Engl 2011, 50, 6527-6529.

23. Armishaw, C. J.; Daly, N. L.; Nevin, S. T.; Adams, D. J.; Craik, D. J.; Alewood, P. F. J Biol Chem 2006, 281, 14136-14143.

24. Blanchfield, J. T.; Gallagher, O. P.; Cros, C.; Lewis, R. J.; Alewood, P. F.; Toth, I. Biochem Biophys Res Commun 2007, 361, 97-102.

25. Blanchfield, J. T.; Dutton, J. L.; Hogg, R. C.; Gallagher, O. P.; Craik, D. J.; Jones, A.; Adams, D. J.; Lewis, R. J.; Alewood, P. F.; Toth, I. J Med Chem 2003, 46, 1266-1272.

26. Blanchfield, J.; Dutton, J.; Hogg, R.; Craik, D.; Adams, D.; Lewis, R.; Alewood, P.; Toth, I. Lett Pept Sci 2001, 8, 235-239.

27. Green, B. R.; Catlin, P.; Zhang, M. M.; Fiedler, B.; Bayudan, W.; Morrison, A.; Norton, R. S.; Smith, B. J.; Yoshikami, D.; Olivera, B. M.; Bulaj, G. Chem Biol 2007, 14, 399-407.

28. Berecki, G.; McArthur, J. R.; Cuny, H.; Clark, R. J.; Adams, D. J. J Gen Physiol 2014, 143, 465-479.

29. Callaghan, B.; Haythornthwaite, A.; Berecki, G.; Clark, R. J.; Craik, D. J.; Adams, D. J. J Neurosci 2008, 28, 10943-10951.

30. Miles, L. A.; Dy, C. Y.; Nielsen, J.; Barnham, K. J.; Hinds, M. G.; Olivera, B. M.; Bulaj, G.; Norton, R. S. J Biol Chem 2002, 277, 43033-43040.

31. Krieger, E.; Koraimann, G.; Vriend, G. Proteins 2002, 47, 393-402.

32. Zoete, V.; Cuendet, M. A.; Grosdidier, A.; Michielin, O. J Comput Chem 2011, 32, 2359-2368.

33. Vanommeslaeghe, K.; Hatcher, E.; Acharya, C.; Kundu, S.; Zhong, S.; Shim, J.; Darian, E.; Guvench, O.; Lopes, P.; Vorobyov, I.; Mackerell, A. D., Jr. J Comput Chem 2010, 31, 671-690.

34. Humphrey, W.; Dalke, A.; Schulten, K. J Mol Graph 1996, 14, 33-38, 27-38.

35. Phillips, J. C.; Braun, R.; Wang, W.; Gumbart, J.; Tajkhorshid, E.; Villa, E.; Chipot, C.; Skeel, R. D.; Kale, L.; Schulten, K. J Comput Chem 2005, 26, 1781-1802.

36. Swedberg, J. E.; de Veer, S. J.; Sit, K. C.; Reboul, C. F.; Buckle, A. M.; Harris, J. M. PLoS One 2011, 6, e19302.

37. Pedretti, A.; Villa, L.; Vistoli, G. J Mol Graph Model 2002, 21, 47-49.

38. Merrifield, R. B. J Am Chem Soc 1963, 85, 2149-&.

39. Schnölzer, M.; Alewood, P.; Jones, A.; Alewood, D.; Kent, S. B. H. Int J Pept Protein Res 1992, 40, 180-193.

40. Pace, C. N.; Vajdos, F.; Fee, L.; Grimsley, G.; Gray, T. Protein Sci 1995, 4, 2411-2423.

41. Vranken, W. F.; Boucher, W.; Stevens, T. J.; Fogh, R. H.; Pajon, A.; Llinas, M.; Ulrich, E. L.; Markley, J. L.; Ionides, J.; Laue, E. D. Proteins 2005, 59, 687-696.

42. Wüthrich, K. NMR of Proteins and Nucleic Acids; Wiley-Interscience: New York, 1986.

43. Wishart, D. S.; Bigam, C. G.; Holm, A.; Hodges, R. S.; Sykes, B. D. J Biomol NMR 1995, 5, 67-81.

44. Wang, C. K.; Northfield, S. E.; Swedberg, J. E.; Colless, B.; Chaousis, S.; Price, D. A.; Liras, S.; Craik, D. J. Eur J Med Chem 2015, 97, 202-213.

45. Dutton, J. L.; Bansal, P. S.; Hogg, R. C.; Adams, D. J.; Alewood, P. F.; Craik, D. J. J Biol Chem 2002, 277, 48849-48857.

46. Wishart, D. S.; Sykes, B. D.; Richards, F. M. J Mol Biol 1991, 222, 311-333.

47. Clark, R. J.; Fischer, H.; Nevin, S. T.; Adams, D. J.; Craik, D. J. J Biol Chem 2006, 281, 23254-23263.

48. Sun, H.; Chow, E. C.; Liu, S.; Du, Y.; Pang, K. S. Expert Opin Drug Metab Toxicol 2008, 4, 395-411.

49. Lennernas, H. J Pharm Pharmacol 1997, 49, 627-638.

50. Artursson, P. J Pharm Sci 1990, 79, 476-482.

51. Yee, S. Pharm Res 1997, 14, 763-766.

52. Kerns, E. H.; Di, L.; Petusky, S.; Farris, M.; Ley, R.; Jupp, P. J Pharm Sci 2004, 93, 1440-1453.

53. Adson, A.; Burton, P. S.; Raub, T. J.; Barsuhn, C. L.; Audus, K. L.; Ho, N. F. J Pharm Sci 1995, 84, 1197-1204.

54. Avdeef, A.; Artursson, P.; Neuhoff, S.; Lazorova, L.; Grasjo, J.; Tavelin, S. Eur J Pharm Sci 2005, 24, 333-349.

55. Hayeshi, R.; Hilgendorf, C.; Artursson, P.; Augustijns, P.; Brodin, B.; Dehertogh, P.; Fisher, K.; Fossati, L.; Hovenkamp, E.; Korjamo, T.; Masungi, C.; Maubon, N.; Mols, R.; Mullertz,

A.; Monkkonen, J.; O'Driscoll, C.; Oppers-Tiemissen, H. M.; Ragnarsson, E. G.; Rooseboom, M.; Ungell, A. L. Eur J Pharm Sci 2008, 35, 383-396.

56. Shirasaka, Y.; Sakane, T.; Yamashita, S. J Pharm Sci 2008, 97, 553-565.

57. Elsby, R.; Surry, D. D.; Smith, V. N.; Gray, A. J. Xenobiotica 2008, 38, 1140-1164.

58. Augustijns, P. F.; Bradshaw, T. P.; Gan, L. S.; Hendren, R. W.; Thakker, D. R. Biochem Biophys Res Commun 1993, 197, 360-365.

59. White, T. R.; Renzelman, C. M.; Rand, A. C.; Rezai, T.; McEwen, C. M.; Gelev, V. M.; Turner, R. A.; Linington, R. G.; Leung, S. S.; Kalgutkar, A. S.; Bauman, J. N.; Zhang, Y.; Liras, S.; Price, D. A.; Mathiowetz, A. M.; Jacobson, M. P.; Lokey, R. S. Nat Chem Biol 2011, 7, 810-817.

Figure Legends

Figure 1. Sequences and structures of cVc1.1 linker analogues. (A) A schematic illustrating the structure of cVc1.1 and its linker analogues. The peptide contains a helical region that is cross-braced by two disulfide bonds in a Cys^{I}-Cys^{III} and Cys^{II}-Cys^{IV} pattern. This disulfide pattern forms two loop sequences between Cys^{II} and Cys^{III} and Cys^{III} and Cys^{IV} as indicated. The N and C termini are then joined by a linker sequence. (B) Sequences of Vc1.1 and its analogues. The conserved cystines are highlighted in yellow and the disulfide bonds and cyclic backbone indicted by the solid black line. The linker sequences for each analogue are shown with *N*-methylated residues underlined and highlighted in green.

Figure 2. Molecular dynamics simulations of cVc1.1 and linker analogues. (A) Ribbon plot of 50 evenly spaced simulation structure frames overlaid with the average simulation structure (left) and overlay of the average simulation structure stick models (right) of cVc1.1 (light blue) with Vc1.1 (pink). Disulfide bonds are shown in yellow, nitrogens in blue and oxygens in red. Ribbon plot of 50 simulation structure frames overlayed with the average simulation structure (left) and overlay of the average simulation structure stick models (right) of cVc1.1 (light blue) with (B) cVc1.1-L1 (pink), (C) cVc1.1-L2 (pink) and (D) cVc1.1-L3 (pink).

Figure 3. Purity and characterisation of cVc1.1 linker analogues. Analytical RP-HPLC chromatograms (left) of cVc1.1-L1 (top), cVc1.1-L2 (middle) and cVc1.1-L3 (bottom) illustrating the high degree of purity and relative hydrophobicity of each peptide. To the right are the corresponding mass spectra for each peptide, which are consistent with the expected molecular weight of the cyclic and oxidised peptides.

Figure 4. Structural studies of cVc1.1 and the linker analogues at 280 K. (A) A comparison of the secondary Hα shifts of cVc1.1 (filled circles), cVc1.1-L1 (crosses), cVc1.1-L2 (open squares), cVc1.1-L3 (open diamonds). The values for each peptide are very similar for each amino acid across the sequence. Some variation is seen for cVc1.1-L2 but this is likely due to the NMR data for this peptide being recorded in 50:50 acetonitrile/water. The loop and linker regions are indicated on the graph. (B) Molecular dynamics simulation of cVc1.1-L2 in 50% acetonitrile. Overlay of the average simulation structure stick models of cVc1.1 simulated in water (light blue) with Vc1.1-L2 simulated in 50% acetonitrile (pink). The structures excluding the linker overlaid with an α-carbon RMSD of 0.69 Å. Disulfide bonds are shown in yellow, nitrogens in blue and oxygens in red.

Figure 5. Stability of cVc1.1 linker analogues in human serum. Linker analogues were tested for their stability in human serum over a 24 h time period. cVc1.1-L3 (open diamonds) was shown to have similar stability to cVc1.1 (filled circles). cVc1.1-L1 (crosses) and L2 (open squares) had a similar stability, which was less stable than cVc1.1-L3 but slightly improved compared to linear Vc1.1 (filled triangles). Data points are means ± SEM from 3−4 separate experiments.

Figure 6. Effect of cVc1.1-L1, cVc1.1-L2 and cVc1.1-L3 peptides on whole-cell calcium channel currents (I_{Ca}) in rat DRG neurons. A, Compounds cVc1.1-L1-3 do not inhibit I_{Ca}. *Left:* Time course of I_{Ca} peak amplitude in the absence (a) and presence of 500 nM cVc1.1-L1-3 (b, c, d) or baclofen (e). I_{Ca} were elicited by 200 ms step depolarizations from a holding potential of −80 mV to 0mV at a frequency of 0.1 Hz. *Right*: representative I_{Ca} traces at the times indicated by lower case letters. Horizontal dotted line indicates zero-current level. Colored bars indicate the duration of cVc1.1-L1-3 or baclofen application. **B**, cVc1.1-L1 (500 nM) has no effect on I_{Ca} amplitude, whereas cVc1.1 (500 nM) inhibits I_{Ca}. Bars indicate cVc1.1-L1 peptide, cVc1.1 or baclofen application (*left*). Experimental procedure and voltage protocol: same as in A. Representative I_{Ba}

traces (*right*) are shown at the times indicated by lowercase letters. Horizontal dotted line represents zero-current level. **C**, Averaged relative peak I_{Ca} amplitudes ($I/I_{control}$) ± SEM in the presence of cVc1.1-L1-3 (500 nM) or baclofen (50 μM). Peak I_{Ca} amplitude was analyzed in the absence and presence of cVc1.1-L1, cVc1.1-L2 or cVc1.1-L3, and subsequently baclofen. Maximum I_{Ca} inhibition with 500 nM cVc1.1-L1 was 6.8 ± 1.3 % (n = 7), whereas cVc1.1-L2 or L3 (500 nM) did not inhibit I_{Ca}. Baclofen (50 μM) inhibited I_{Ca} by 34.9 ± 4 % (n = 7).

Table 1. Molecular dynamics simulation

Linker analogues[a,b]	Intramolecular Hydrogen Bonds	α-Carbon RMSD Values (Å)[c]
cVc1.1		
GGAAGG	7.56 ± 0.13	-
Single residue *N*-methylation		
GGAAGG	7.99 ± 0.34	0.80
G**G**AAGG	7.25 ± 0.20	0.30
GG**A**AGG	7.55 ± 0.26	0.73
GGA**A**GG	8.39 ± 0.71	0.40
GGAA**G**G	7.85 ± 0.12	0.50
GGAAG**G**	5.98 ± 0.12	0.31
Hydrophobic residues		
GGLL**GG**	7.04 ± 0.39	0.95
GG**LL**GG	8.20 ± 0.30	0.82
GL**G**L**G**L	6.96 ± 0.05	0.64
G**L**PG**L**P	6.56 ± 0.62	0.56
G**V**G**V**GV	7.22 ± 0.13	0.26
Basic residues		
GKG**K**GK	7.25 ± 0.41	0.69
GK**G**K**G**K	6.95 ± 0.42	0.65
G**K**PG**K**P	6.86 ± 0.55	0.65
GGKK**GG**	7.28 ± 0.06	0.62
G**K**G**K**G**K**	6.43 ± 0.30	0.48
GK**G**KGK	8.06 ± 0.08	0.33
Acidic residues		
GG**D**D**G**G	7.47 ± 0.16	0.78
GD**G**D**G**D	6.7 8± 0.10	0.55
GE**G**E**G**E	8.17 ± 0.12	0.24

[a] Sequences are GCCSDPRCNYDHPEIC-XXXXXX where X represents the linker sequences

[b] *N*-methylated residues are highlighted in bold font

[c] α-Carbon RMSD excludes the linker

Table 2. Caco-2 and PAMPA permeability and *in silico* calculated biophysical parameters

Compound	Caco-2 permeability x 10^6 ± SEM (cm/s^{-1})	PAMPA permeability X 10^6 ± SEM (cm/s^{-1})	PSA ± SD[b]	SA ± SD[b]	vLogP ± SD[b]
Atenolol	0.275 ± 0.125	0.033 ± 0.011	166	570	1.5
Quinidine	17.330 ± 0.675	6.140 ± 0.580	67	575	2.6
cVc1.1	nd[a]	0.008 ± 0.004	814 ± 32	1878 ± 50	-9.1 ± 0.5
cVc1.1-L1	nd[a]	nd[a]	960 ± 57	2236 ± 80	-17.1 ± 0.9
cVc1.1-L2	0.367 ± 0.200	0.006 ± 0.005	713 ± 33	2040 ± 34	-5.4 ± 0.4
cVc1.1-L3	nd[a]	0.005 ± 0.004	1004 ± 39	2091± 44	-10.8 ± 0.6

PSA: polar surface area, SA: surface area, vLogP: virtual log water/octanol partitioning coefficient

[a] Non-detectable

[b] Standard deviations do not apply to atenolol and quinidine calculated from a single structure

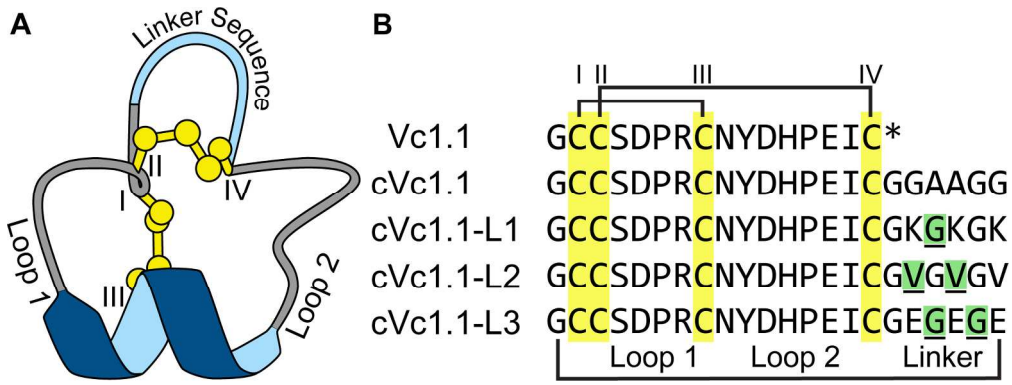

Figure 1. Sequences and structures of cVc1.1 linker analogues. (A) A schematic illustrating the structure of cVc1.1 and its linker analogues. The peptide contains a helical region that is cross-braced by two disulfide bonds in a CysI-CysIII and CysII-CysIV pattern. This disulfide pattern forms two loop sequences between CysII and CysIII and CysIII and CysIV as indicated. The N and C termini are then joined by a linker sequence. (B) Sequences of Vc1.1 and its analogues. The conserved cystines are highlighted in yellow and the disulfide bonds and cyclic backbone indicted by the solid black line. The linker sequences for each analogue are shown with N-methylated residues underlined and highlighted in green.
191x71mm (300 x 300 DPI)

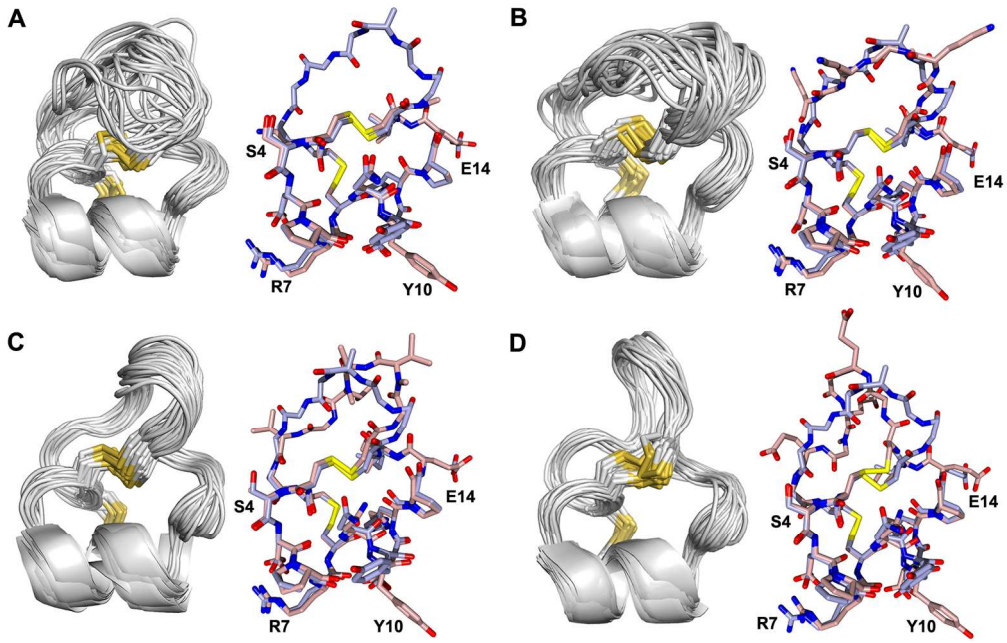

Figure 2. Molecular dynamics simulations of cVc1.1 and linker analogues. (A) Ribbon plot of 50 evenly spaced simulation structure frames overlaid with the average simulation structure (left) and overlay of the average simulation structure stick models (right) of cVc1.1 (light blue) with Vc1.1 (pink). Disulfide bonds are shown in yellow, nitrogens in blue and oxygens in red. Ribbon plot of 50 simulation structure frames overlayed with the average simulation structure (left) and overlay of the average simulation structure stick models (right) of cVc1.1 (light blue) with (B) cVc1.1-L1 (pink), (C) cVc1.1-L2 (pink) and (D) cVc1.1-L3 (pink).
169x107mm (300 x 300 DPI)

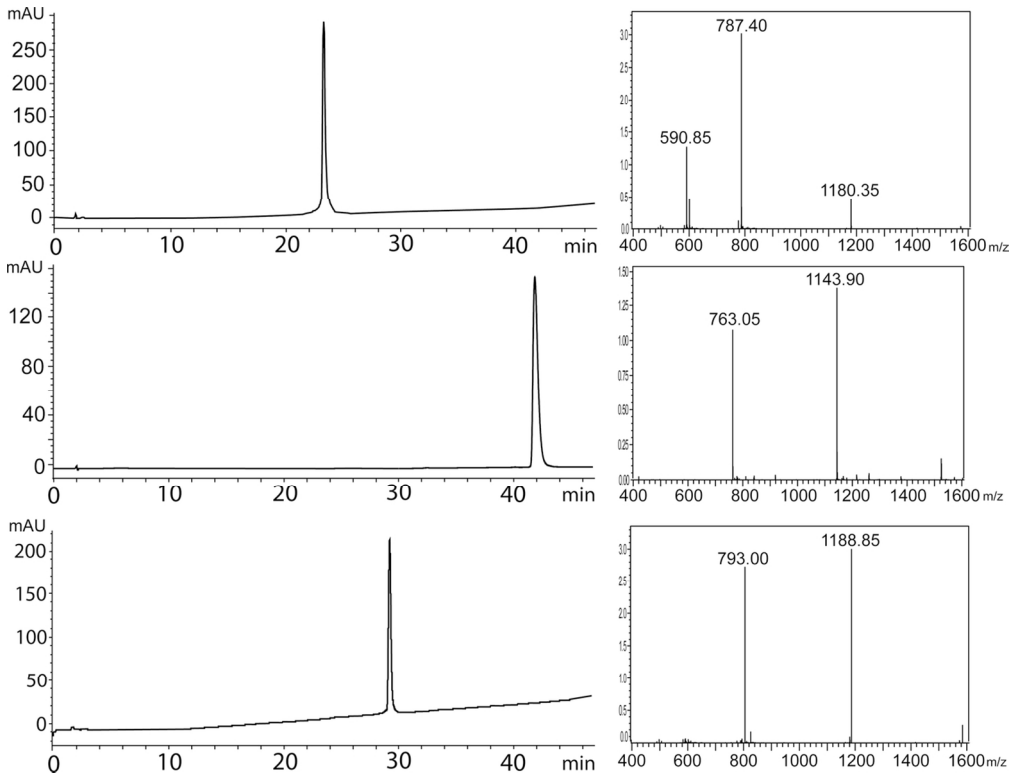

Figure 3. Purity and characterisation of cVc1.1 linker analogues. Analytical RP-HPLC chromatograms (left) of cVc1.1-L1 (top), cVc1.1-L2 (middle) and cVc1.1-L3 (bottom) illustrating the high degree of purity and relative hydrophobicity of each peptide. To the right are the corresponding mass spectra for each peptide, which are consistent with the expected molecular weight of the cyclic and oxidised peptides.
122x93mm (300 x 300 DPI)

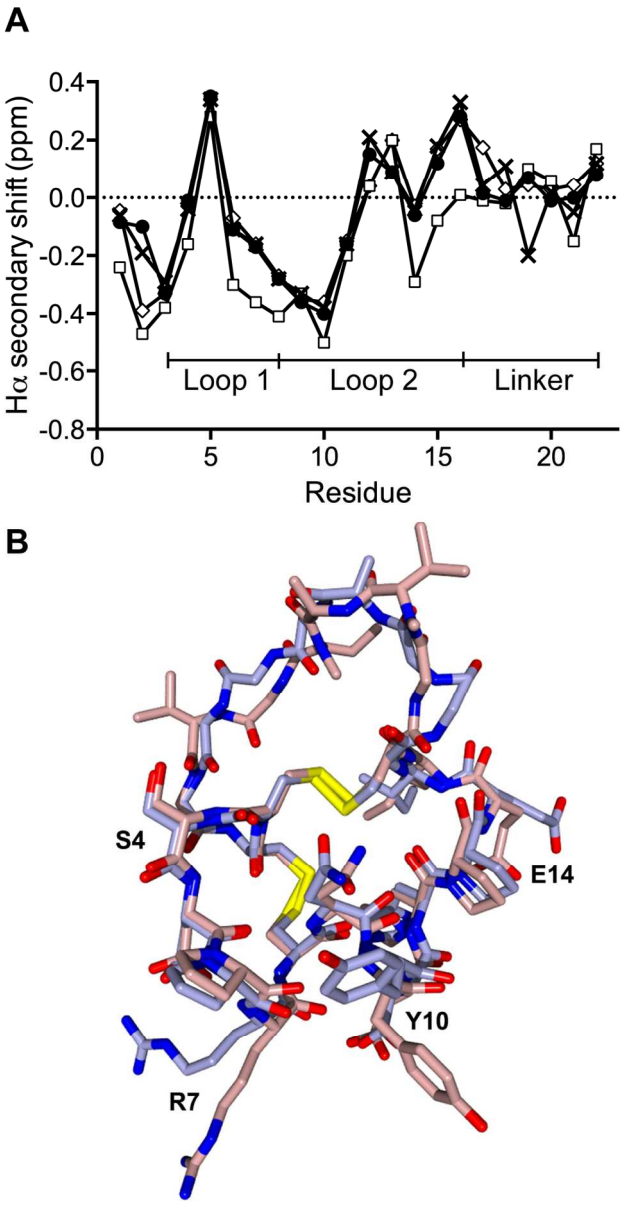

Figure 4. Structural studies of cVc1.1 and the linker analogues at 280 K. (A) A comparison of the secondary Hα shifts of cVc1.1 (filled circles), cVc1.1-L1 (crosses), cVc1.1-L2 (open squares), cVc1.1-L3 (open diamonds). The values for each peptide are very similar for each amino acid across the sequence. Some variation is seen for cVc1.1-L2 but this is likely due to the NMR data for this peptide being recorded in 50:50 acetonitrile/water. The loop and linker regions are indicated on the graph. (B) Molecular dynamics simulation of cVc1.1-L2 in 50% acetonitrile. Overlay of the average simulation structure stick models of cVc1.1 simulated in water (light blue) with Vc1.1-L2 simulated in 50% acetonitrile (pink). The structures excluding the linker overlaid with an α-carbon RMSD of 0.69 Å. Disulfide bonds are shown in yellow, nitrogens in blue and oxygens in red.
91x175mm (300 x 300 DPI)

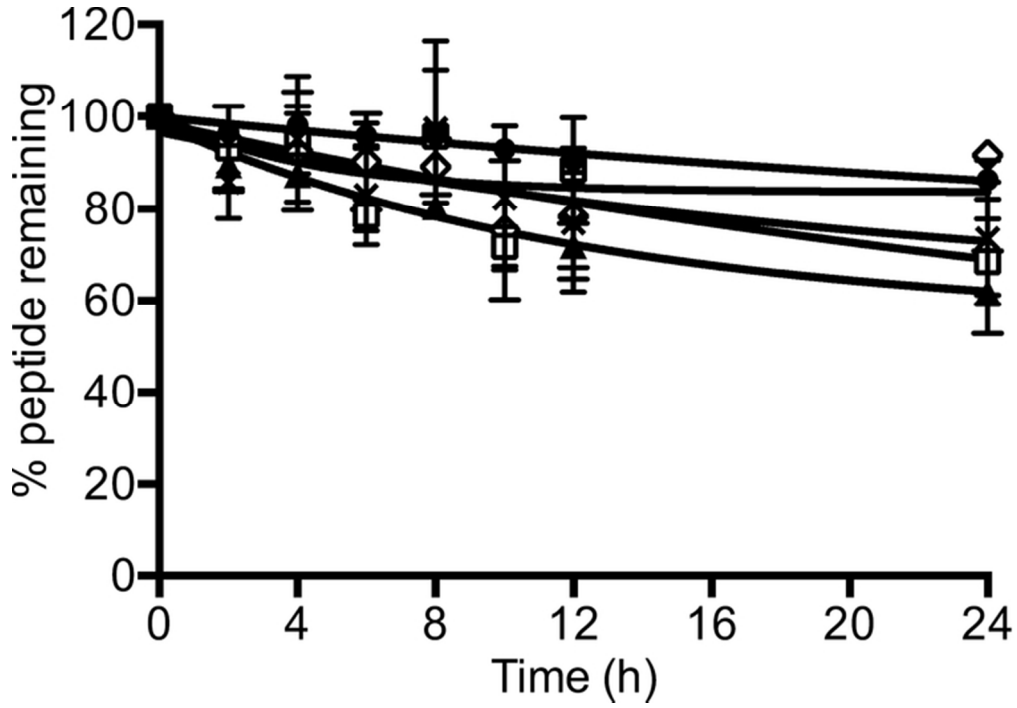

Figure 5. Stability of cVc1.1 linker analogues in human serum. Linker analogues were tested for their stability in human serum over a 24 h time period. cVc1.1-L3 (open diamonds) was shown to have similar stability to cVc1.1 (filled circles). cVc1.1-L1 (crosses) and L2 (open squares) had a similar stability, which was less stable than cVc1.1-L3 but slightly improved compared to linear Vc1.1 (filled triangles). Data points are means ± SEM from 3−4 separate experiments.
63x44mm (300 x 300 DPI)

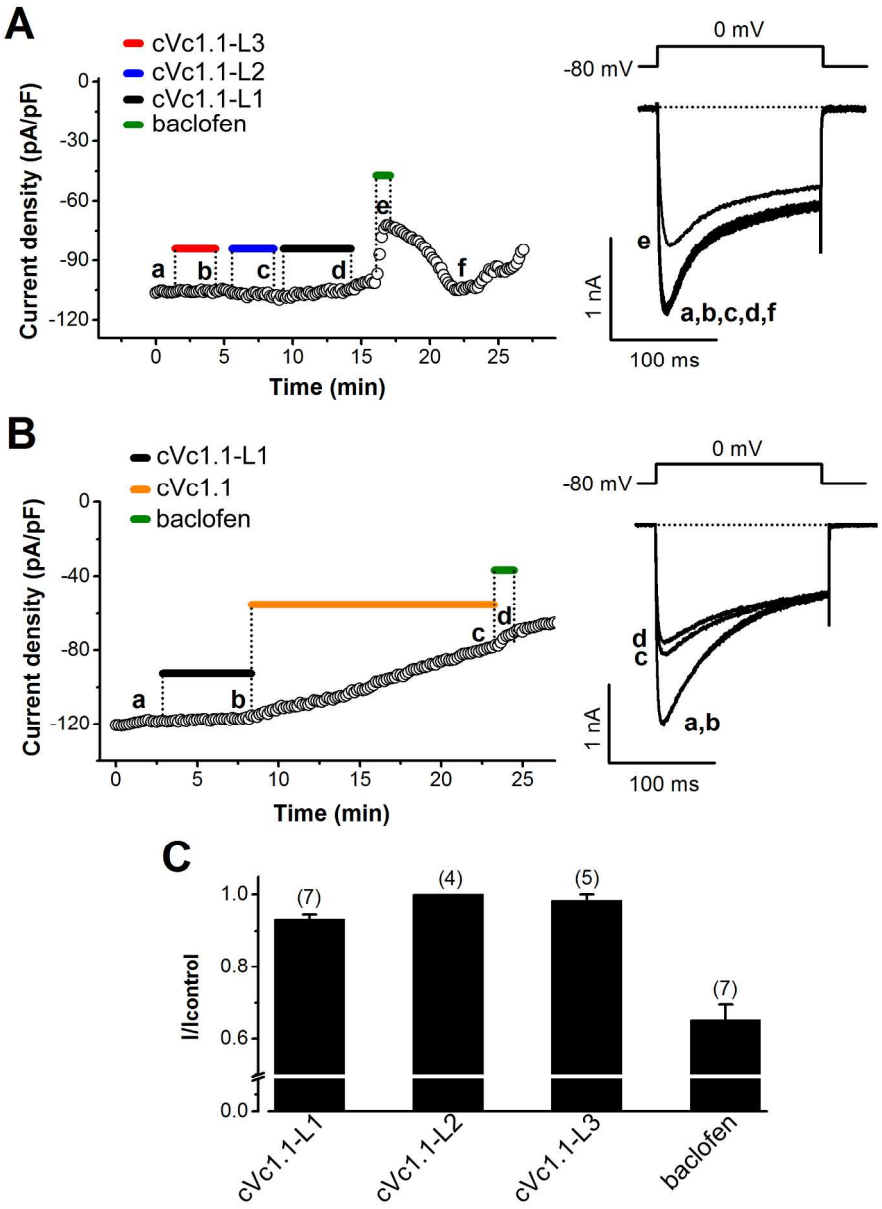

Figure 6. Effect of cVc1.1-L1, cVc1.1-L2 and cVc1.1-L3 peptides on whole-cell calcium channel currents (ICa) in rat DRG neurons. (A), Compounds cVc1.1-L1-3 do not inhibit ICa. Left: Time course of ICa peak amplitude in the absence (a) and presence of 500 nM cVc1.1-L1-3 (b, c, d) or baclofen (e). ICa were elicited by 200 ms step depolarizations from a holding potential of −80 mV to 0mV at a frequency of 0.1 Hz. Right: representative ICa traces at the times indicated by lower case letters. Horizontal dotted line indicates zero-current level. Colored bars indicate the duration of cVc1.1-L1-3 or baclofen application. (B), cVc1.1-L1 (500 nM) has no effect on ICa amplitude, whereas cVc1.1 (500 nM) inhibits ICa. Bars indicate cVc1.1-L1 peptide, cVc1.1 or baclofen application (left). Experimental procedure and voltage protocol: same as in A. Representative IBa traces (right) are shown at the times indicated by lowercase letters. Horizontal dotted line represents zero-current level. (C), Averaged relative peak ICa amplitudes (I/Icontrol) ± SEM in the presence of cVc1.1-L1-3 (500 nM) or baclofen (50 µM). Peak ICa amplitude was analyzed in the absence and presence of cVc1.1-L1, cVc1.1-L2 or cVc1.1-L3, and subsequently baclofen. Maximum ICa inhibition with 500 nM cVc1.1-L1 was 6.8 ± 1.3 % (n = 7), whereas cVc1.1-L2 or L3 (500 nM) did not inhibit ICa.

Baclofen (50 μM) inhibited ICa by 34.9 ± 4 % (n = 7).
171x235mm (300 x 300 DPI)

Author/s:
Carstens, BB; Swedberg, J; Berecki, G; Adams, DJ; Craik, DJ; Clark, RJ

Title:
Effects of Linker Sequence Modifications on the Structure, Stability, and Biological Activity of a Cyclic alpha-Conotoxin

Date:
2016-11-01

Citation:
Carstens, B. B., Swedberg, J., Berecki, G., Adams, D. J., Craik, D. J. & Clark, R. J. (2016). Effects of Linker Sequence Modifications on the Structure, Stability, and Biological Activity of a Cyclic alpha-Conotoxin. BIOPOLYMERS, 106 (6), pp.864-875. https://doi.org/10.1002/bip.22848.